

Fig. 2—Input VSWR as a function of  $Z_1/Z_0$  ( $Q_L=100$ ).

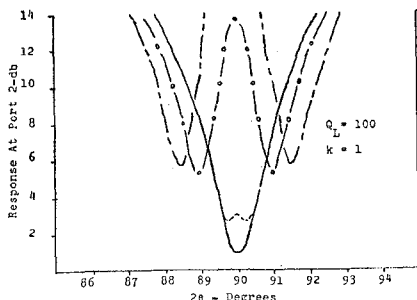


Fig. 3—Port 2 response ( $Q_L=100$ ).

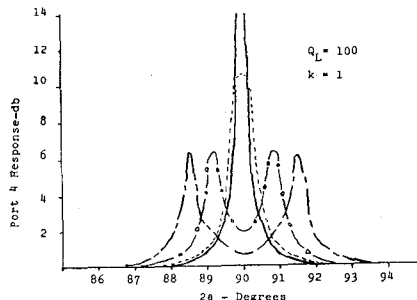


Fig. 4—Port 4 response ( $Q_L=100$ ).

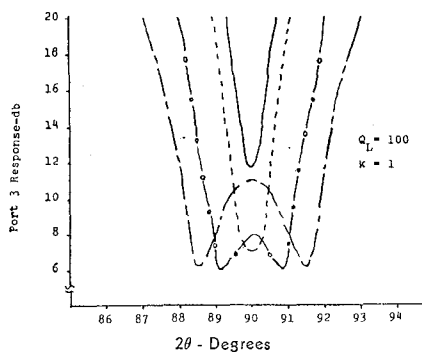


Fig. 5—Port 3 response ( $Q_L=100$ ).

Plots such as those shown in Figs. 2-5 are of value in two possible ways. If a particular type of discontinuity such as a dielectric post exists in the loop sides, then a knowledge of the discontinuity equivalent circuit permits calculation of  $Z_I$  and  $\beta_I$  used above. Thus the discontinuity effects are readily taken into account, and the resulting frequency response is predictable. Secondly, plots of the above form can serve as aids to empirical adjustment by comparing the measured response to the predicted. In this case the required assumption is that the

variation of  $Z_I$  is negligible over the frequency band of interest.

In summary, equations for the transmission and reflection coefficients for the single resonator traveling wave filter have been presented for the case where the loop sides have an arbitrary characteristic impedance. It has been shown that when  $Z_I \neq Z_0$  ideal directional filter characteristics are not attainable.<sup>2</sup> The effects on frequency response are in qualitative agreement with those observed experimentally. Also  $\beta_I \neq 2\theta$  cause a predictable frequency shift.

ROBERT D. STANDLEY  
A. C. TODD  
IIT Research Institute  
Chicago, Ill.

<sup>2</sup> F. S. Coale, "A Traveling-Wave Directional," IRE TRANS. ON MICROWAVE THEORY AND TECHNIQUES, vol. MTT-4, pp. 256-260; October, 1956.

### A Wall-Current Detector for Use with Beam Waveguides\*

A crystal detector mount which is well suited for use with beam waveguides<sup>1</sup> of either the refracting or reflecting type is based on the same concept as the wall-current detector of deRonde.<sup>2</sup> The geometry of one form of the detector is shown in Fig. 1.

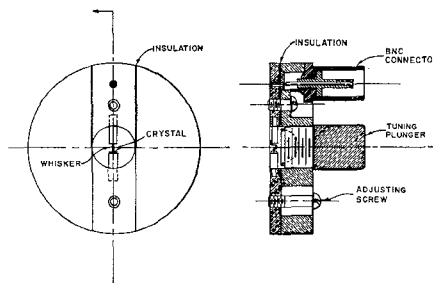


Fig. 1—Schematic drawing of a wall-current detector for use with beam waveguides.

Radiation incident on the detector with its magnetic intensity horizontally polarized causes a vertical surface current to flow, some of which passes through the rectifying junction mounted across the circular aperture. A tuning plunger mounted behind the rectifying junction is used in the conventional manner to tune the detector. A dielectric lens may be used directly in front of the detector to concentrate the incident radiation on the diode.

A detector of this type has been used for making measurements on a 70-Gc beam

\* Received July 31, 1963. Work supported by the United States Air Force, Rome Air Development Center, Contract AF 30(602)-3046 (Richard F. Davis).

<sup>1</sup> G. Goubau and F. Schwering, "On the Guided propagation of electromagnetic wave beams," IRE TRANS. ON ANTENNAS AND PROPAGATION, vol. AP-9, pp. 248-256; May, 1961.

<sup>2</sup> F. C. deRonde, "A Universal Wall-Current Detector," presented at Millimeter and Submillimeter Conf., January 7-10, 1963, Orlando, Fla.

waveguide. Using relatively crude assembly techniques it is possible to construct units with an output voltage of the order of 15 millivolts per milliwatt of power in the radiation beam, which has a minimum cross-sectional area of approximately 6 square centimeters.

M. D. SIRKIS  
C. S. KIM  
Ultramicrowave Group  
Dept. of Electrical Engineering  
University of Illinois  
Urbana, Ill.

### Solution of the Fourier Heat Flow Equation in Waveguides Filled with Lossy Dielectrics\*

The temperature distribution within a waveguide filled with a lossy dielectric, and propagating a specified mode, may be conveniently obtained by the Green's function method. Such a solution is useful for describing the temperature distribution in vacuum windows, for example.

The temperature distribution in the steady state is given by Fourier's equation

$$\kappa \nabla^2 T + \dot{p} = 0 \quad (1)$$

where  $\kappa$  is the thermal conductivity and  $T$  the temperature of the material. A spontaneous source of heat power per unit volume  $\dot{p}$  is supposed. In the example considered here, the heat power is presumed to be generated by some mechanism as molecular friction due to oscillation of the dipolar material attempting to align itself with the electric field of an RF wave. This heat will establish a thermal gradient in the dielectric material as it flows toward a heat sink, which will constitute a boundary condition on the differential equation. We will not consider temperature variations along the axis of the waveguide, which is equivalent to assuming that the loss per unit length along the axis is small. Therefore we will only require a solution of Poisson's equation (and a Green's function) in two dimensions.

To illustrate the explanation we consider the case of the cylindrical TE<sub>11</sub> mode, for which the field description is given to sufficient accuracy by the solution of the homogeneous wave equation (1):

$$E_r = \frac{2E_0}{k_{\rho r}} J_1(k_{\rho r}) \sin \phi_j \exp j(\omega t - \beta z)$$

$$E_{\phi} = 2E_0 J_1'(k_{\rho r}) \cos \phi_j \exp j(\omega t - \beta z) \quad (2)$$

where  $E_0$  is the maximum field intensity at the origin. Thus, the heat power source function is given by

$$p(r, \phi) = \frac{\sigma E^2}{2} = \frac{\sigma E_0^2}{2} [J_0^2(k_{\rho r}) + J_2^2(k_{\rho r}) - 2J_0(k_{\rho r})J_2(k_{\rho r}) \cos 2\phi] \quad (3)$$

\* Received June 17, 1963; revised manuscript received August 7, 1963.

where elementary identities have been used to convert the Bessel functions into a form suitable for integration. The dielectric conductivity  $\sigma = \omega \epsilon''$ , where  $\epsilon = \epsilon' + \epsilon''$  is the complex permittivity and is related to the loss tangent by  $\tan \delta = \epsilon''/\epsilon'$ .

The cylindrical Green's function is well known (2);

$$\begin{aligned} \frac{1}{2}G_1 &= \ln \frac{a}{r} - \sum \frac{1}{n} \left( \frac{r_0^{2n}}{a^{2n}} - \frac{r_0^n}{r^n} \right) \\ &\cdot \cos n(\phi_0 - \phi) \quad r > r_0 \\ \frac{1}{2}G_2 &= \ln \frac{a}{r_0} - \sum \frac{1}{n} \left( \frac{r_0^{2n}}{a^{2n}} - \frac{r^n}{r_0^n} \right) \\ &\cdot \cos n(\phi_0 - \phi) \quad r < r_0 \end{aligned} \quad (4)$$

where  $r, \phi$  refers to field points and  $r_0, \phi_0$  to source points. At  $r=a, T=0$ . The heat flow equation may now be put in the form of the solution

$$\begin{aligned} T(r, \phi) &= \frac{1}{2\pi\kappa} \int_0^{2\pi} \left[ \int_0^r r_0 G_1 p(r_0, \phi_0) dr_0 \right. \\ &\left. + \int_r^a r_0 G_2 p(r_0, \phi_0) dr_0 \right] d\phi_0. \end{aligned} \quad (5)$$

Performing the indicated integrations and combining terms,

$$\begin{aligned} \frac{2\kappa}{\sigma E_0^2} T(r, \phi) &= r^2 \left[ \left( \frac{1}{k_c^2 r^2} - 1 \right) (J_0^2(k_c r) + J_1^2(k_c r)) \right. \\ &+ \frac{1}{2k_c r} J_0(k_c r) J_1(k_c r) \left. \right] \\ &- a^2 \left[ \left( \frac{1}{k_c^2 a^2} - 1 \right) (J_0^2(k_c a) + J_1^2(k_c a)) \right. \\ &+ \frac{1}{2k_c a} J_0(k_c a) J_1(k_c a) \left. \right] \\ &- \frac{r^2}{6} \left[ \left( \frac{4}{k_c^2 r^2} + 1 \right) J_1^2(k_c r) - 2J_0^2(k_c r) \right. \\ &+ \frac{2}{k_c r} J_0(k_c r) J_1(k_c r) \\ &- \left( \frac{4}{k_c^2 a^2} + 1 \right) J_1^2(k_c a) + 2J_0^2(k_c a) \\ &- \left. \frac{2}{k_c a} J_0(k_c a) J_1(k_c a) \right] \cos 2\phi. \end{aligned} \quad (6)$$

The power flux, obtained by taking the time average of the Poynting vector over the cross section of the waveguide, may be shown to be

$$\begin{aligned} P &= \pi E_0^2 a^2 J_1^2(k_c a) \left( 1 - \frac{1}{k_c^2 a^2} \right) \\ &\cdot \sqrt{1 - (\lambda/\lambda_c)^2}. \end{aligned} \quad (7)$$

From this expression and the boundary condition for this mode,  $k_c a = 1.84$ , the central temperature may be determined:

$$T_0 = 0.4350 \frac{\sigma \eta P}{\kappa \sqrt{1 - (\lambda/\lambda_c)^2}}. \quad (8)$$

The temperature distribution is shown in Fig. 1.

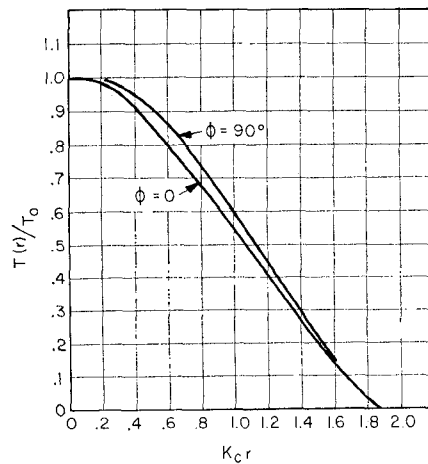


Fig. 1—Normalized temperature distribution for limiting cases.

ACKNOWLEDGMENT

The writer desires to acknowledge helpful discussions with Dr. R. V. Yadavalli during preparation of this note.

WILLIAM J. GALLAGHER  
Litton Industries  
San Carlos, Calif.

REFERENCES

- [1] S. Ramo and J. Whinnery, "Field and Waves in Modern Radio," John Wiley and Sons, Inc., New York, N. Y., p. 336; 1944.
- [2] W. R. Smythe, "Static and Dynamic Electricity," McGraw-Hill Book Co., Inc., New York, N. Y., p. 65; 1950.

A Vacuum Forming Technique for the Fabrication of Spherical or Prolate Spheroidal Reflectors\*

A quick and inexpensive way of making spherical or prolate spheroidal reflectors for use in the millimeter wave range has been developed. This technique is based upon the fact that for small deflections a circular membrane stretched uniformly by a vacuum assumes approximately the shape of a spherical cap, and an elliptical membrane assumes approximately the shape of a prolate spheroidal cap. In making the reflectors, 0.001-inch aluminum foil is used as the membrane because of its low elastic limit. Once the foil is stretched, it retains its shape, eliminating the need for continual pumping.

A cross-sectional view of the apparatus used in making the reflectors is shown in Fig. 1. The vacuum table is  $\frac{3}{8}$ -inch thick aluminum and is fitted with a micrometer in the center. The aluminum foil is cemented to the reflector frame with an industrial adhesive, Eastman 910.<sup>1</sup> The reflector frame is insulated from the vacuum table so that the electrical connection made when the foil touches the micrometer post can be used to actuate a vacuum valve to stop the forming

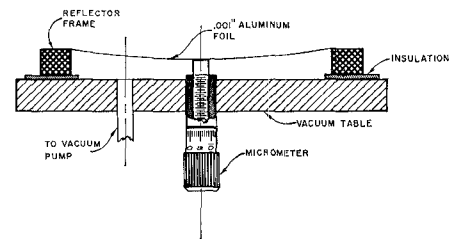


Fig. 1—Cross-sectional view of reflector fabrication apparatus.

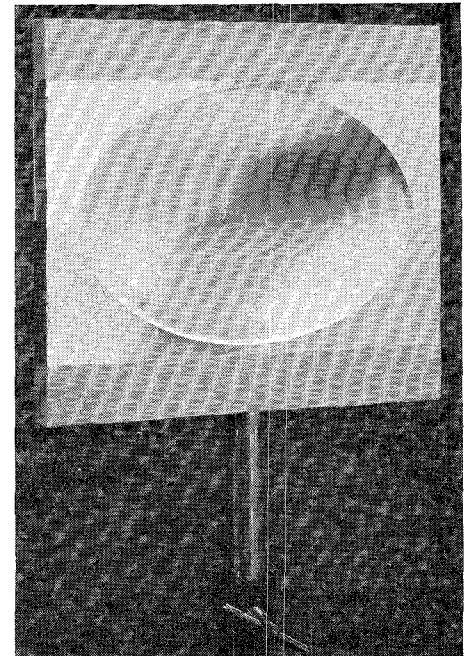


Fig. 2—Prolate spheroidal reflector.

process. This arrangement provides a means for accurately forming the foil to the correct depth.

The construction of the various parts is quite simple with the exception of the reflector frames when prolate spheroidal reflectors are being made. For this case elliptical holes must be cut in the frames, and to do this with a conventional milling machine requires that the frames be made in two sections. By tilting the vertical head of the mill at the correct angle, a fly cutter can be used to cut a semi-ellipse in each half of the frame and the two sections can then be rejoined using, for example, Eastman 910 cement. A completed prolate spheroidal reflector is shown in Fig. 2.

The curvature of the reflectors formed in this way was checked using templates and found to be sufficiently close to the calculated shape for use at the design wavelength of 4 mm. There tend to be small wrinkles at the edge of the foil due to uneven spreading of the adhesive, but these can be allowed for by making the reflectors slightly oversize. The depth of several different reflectors can easily be kept uniform to a tolerance of  $\pm 0.001$ -inch.

J. E. DEGENFORD  
M. D. SIRKIS  
Ultramicrowave Group  
Dept. of Electrical Engineering  
University of Illinois  
Urbana, Ill.

\* Received August 5, 1963. The research reported in this paper was sponsored by the U. S. Air Force, under RADC Contract AF 30(602)-3046 with the University of Illinois, Urbana, Ill.  
<sup>1</sup> A product of Tennessee Eastman Co., Kingsport, Tenn.